Investigation of an autarkic mini wind turbine

Beller, Christina

Published in:
EWEC 2009 Proceedings online

Publication date:
2009

Document Version
Publisher's PDF, also known as Version of record

INVESTIGATION OF AN AUTARKIC MINI WIND TURBINE

Christina Beller
Risø National Laboratory for Sustainable Energy, Technical University of Denmark
cbel@risoe.dtu.dk

Abstract:

In order to enter the urban environment with wind energy applications, a small-scale wind turbine was investigated. Mounted on, e.g. a bike, the citizen is cycling and generating most of the wind. While the bike is parked and wind is blowing, energy is produced, meant to charge small electrical items. Compared to big scale wind turbines, different boundary conditions must be considered. For use in the first experiments, a 24V DC motor was used as generator. The characteristics in generator mode were obtained by connecting it to a motor of the same type. Based on this generator a few different rotor designs were carried out and manufactured.
Keywords: small-scale wind turbine, closed system, battery charger, rotor design

1 Introduction

Small turbine battery charging systems are known and have been used in the maritime environment for some years already. Since a while small turbines started to enter the urban space. The implementation of wind energy in cities is a controversial topic though. Most essential for a success seems to be matter of cost, efficiency, safety and aesthetics. With these thoughts in mind and the idea to introduce wind turbines in a very unobtrusive small scale, initiated this work.
Based on generator characteristics, obtained by measurements, different rotor design parameters were investigated with the help of the design tool developed by Risø DTU, HAWTOPT [1]. Starting point for the rotor layout was a flat, slender plate to be twisted in a certain way and with that simple to produce (see Figure 1). With the aim to reach power coefficients, C_P, able to deliver sufficient power to the generator shaft, variation on parameter constraints followed, like various twist distributions, chord distributions and rotor diameters, *d*, but also parameters like the design tip speed ratio, TSR_{design}, and last but not least the design angle of attack, aoa_{design}, were investigated.

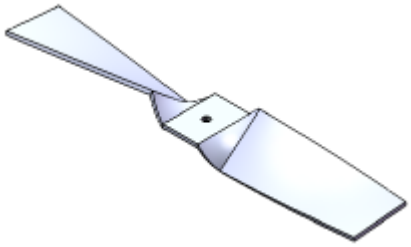

Figure 1: Flat, twisted plate as starting point

There is a short description of the generator characteristics and how they were obtained in the Methods section. Also, the parameter constraints are described in more detail, as well as what happens to C_P when the rotor is designed for lower TSR. The final design, manufactured with a three dimensional printer, is described in the Results section. In the Discussion section the final design will be argued in comparison to the other probably more efficient but not chosen layouts, whereas in the Conclusion section the results meaning for the future of the Mini Wind Turbine are summarized.

As airfoil the NACA0012 airfoil was selected, since it is symmetric and thick enough to be approached from a flat plate (f. e. chord length of 30mm corresponds to a thickness of 3.6mm). The airfoil characteristics predicted by xfoil6.96 are plotted in the following section.

2 Methods

The restricting parameters were a max rotational speed of 2000rpm, a design wind speed of 7m/s, corresponding to a bike speed of 25km/h without additional wind, and the generator shaft diameter with 4mm limiting the maximum rotor diameter with a rule of thumb to approximately 0.40m.
In the following the characteristics for the generator and airfoil are described and the way

to find different rotor design and their individual properties.

2.1 Airfoil

As airfoil a NACA0012 was chosen and aerodynamic data obtained with xfoil6.96 [2] for low Reynolds number ranging between 20.000 and 80.000. Figure 2 shows the found values.

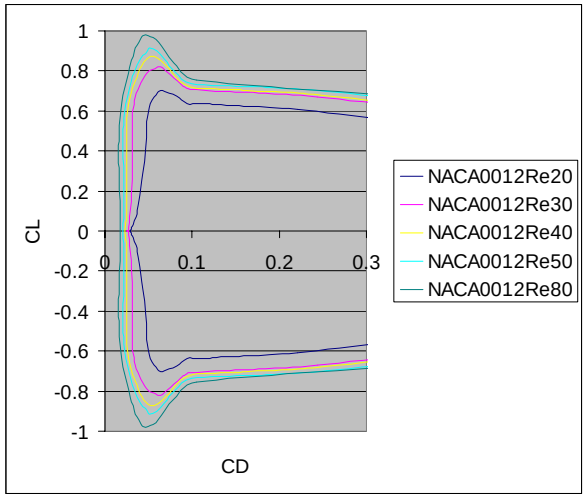

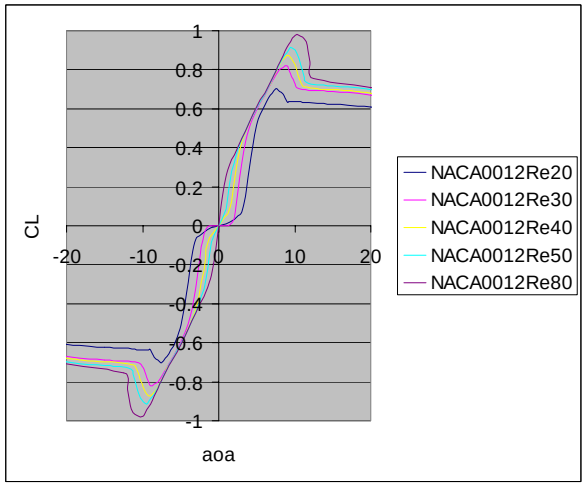

Figure 2: NACA0012; *CL* over *CD; CL* over *aoa*

2.2 Generator

Two 24V direct current motors were connected stiffly at their axes, while one was operating in motor mode, driving the other in generator mode (see Figure 3). Find the motor data sheet in the appendix. In this way the input power for different rotational speed was measured.

Figure 3: Two motors stiffly connected on their axes

With different experimental set-ups, see Figure 4, the power used by the motor itself, the mechanical resistance of the generator and the additional electric resistance, depending on the connected resistor load, 10Ohm, 5.6Ohm, 2.7Ohm, 0.49Ohm, were ascertained and are plotted in Figure 5.

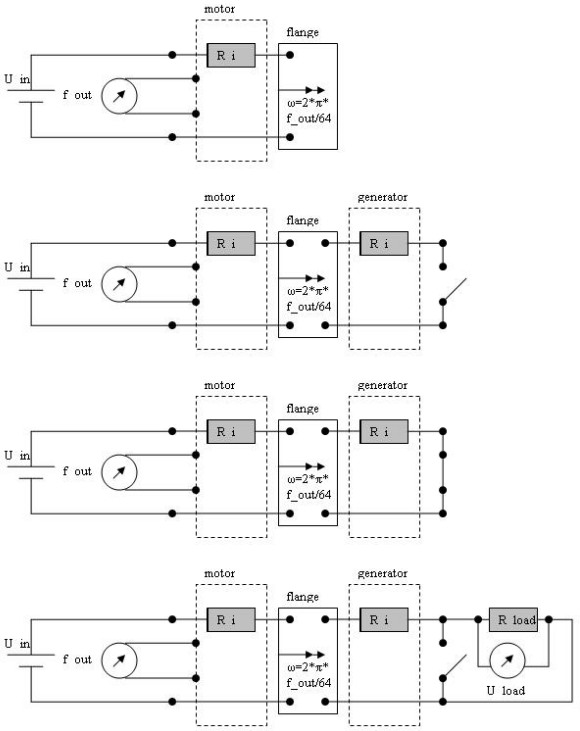

Figure 4: Experimental set-ups for generator

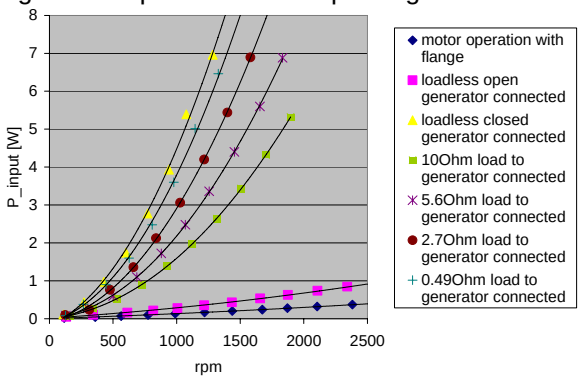

Figure 5: Motor input power over rotational speed

In the next step a rotor design delivering the power to the generator shaft was investigated.

2.3 Rotor Design

With the design tool developed by Risø DTU, HAWTOPT, and the airfoil data from xfoil6.96 different constrained configurations were found and modified in order to approach the generator demand when a 10Ohm resistor is connected. Design variables were

1. shape constraints and number of blades, *n*,
2. design tip speed ratio, TSR_{design},

3. rotor diameter, *d*, and
4. design angle of attack, aoa_{design}.

The first settings were

d:		0.20m
TSR_{design}:		3.0
n:		2

with the modifications

1a)	chord distribution:	linear
	twist distribution:	linear
1b)	chord distribution:	Bezier
	twist distribution:	Bezier
1c) as a) but *n*:		3

The blade designed for a wind speed of 7m/s was then theoretically exposed to different rotational speeds at 7m/s and the same was done for various wind speeds. On the right the colour code is shown. The design point is marked with a big red dot.

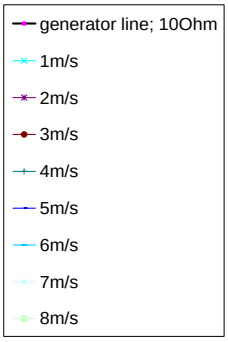

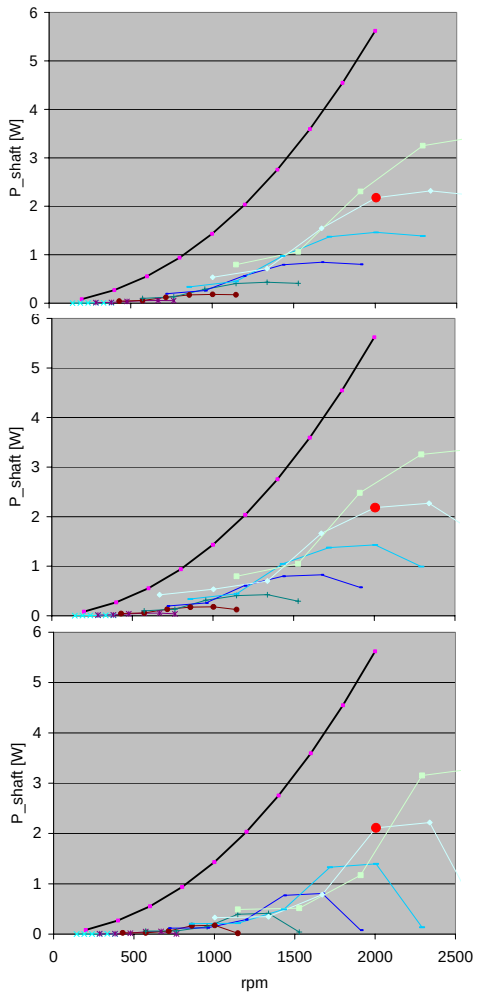

Figure 6: Shape contraint modulation; *P_shaft* over *rpm*

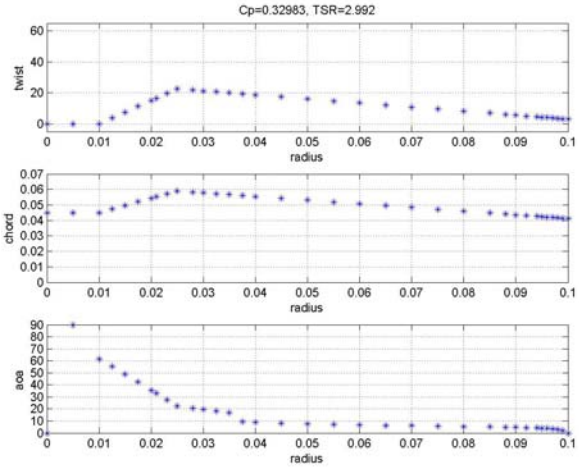

Figure 7: Case 1a); top plot: twist distribution; mid plot: chord distribution; bottom plot: aoa_{design}

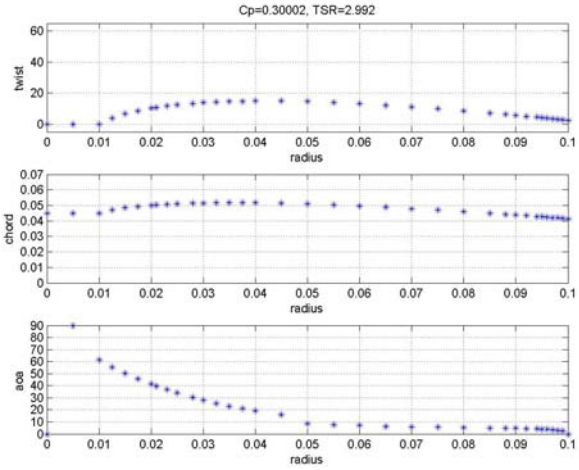

Figure 8: Case 1b); top plot: twist distribution; mid plot: chord distribution; bottom plot: aoa_{design}

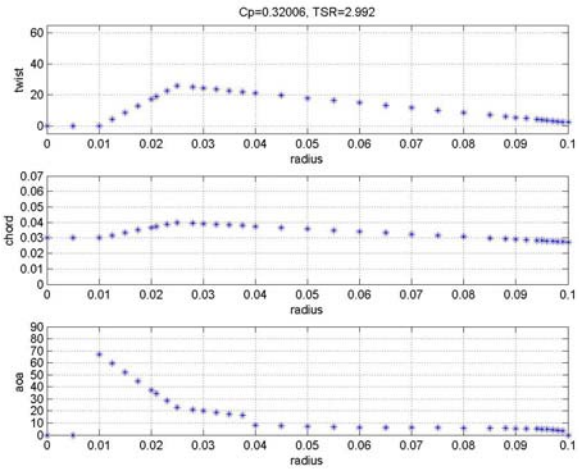

Figure 9: Case 1c); top plot: twist distribution; mid plot: chord distribution; bottom plot: aoa_{design}

In general, the modulations shown in the above plots did not push the rotor power lines closer to the generator line.

Second settings were as 1a) with modulations

1a) TSR_{design}: 3.0
2b) TSR_{design}: 2.0
2c) TSR_{design}: 1.5

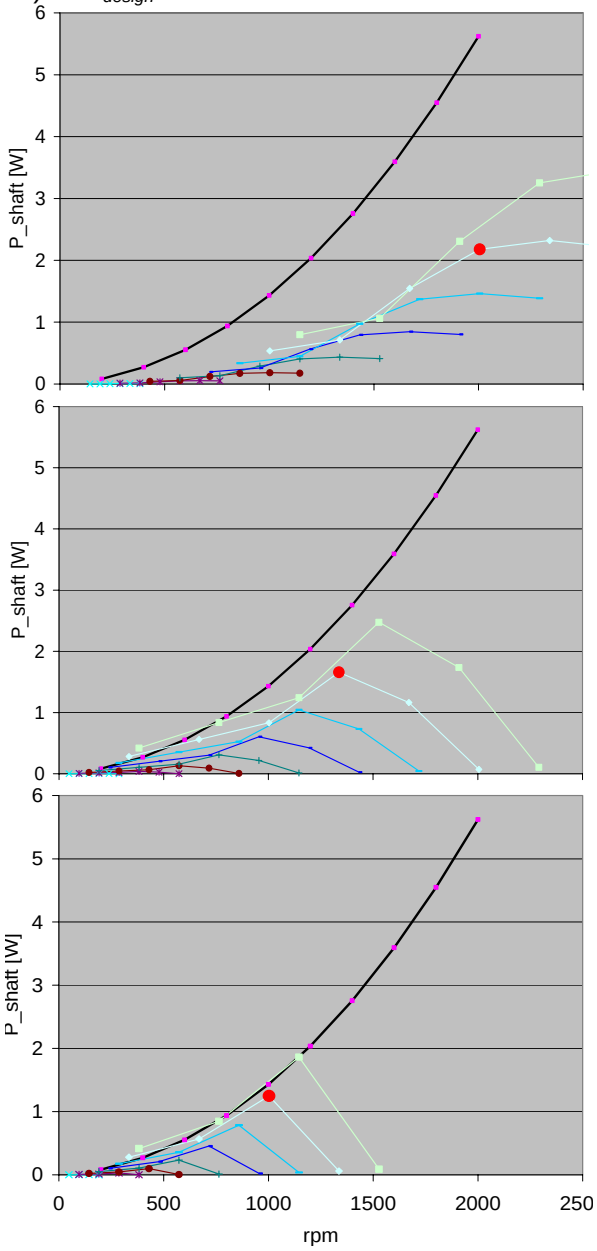

Figure 10: TSR_{design} modulation; *P_shaft* over *rpm*

By changing the design tip speed ratio settings the rotor power curves approach the generator line (see Figure 10) while the C_P value at the design point, $C_{Pdesign}$, red dot, decreases significantly ($C_{Pdesign}(2a)$=0.33; $C_{Pdesign}(2b)$=0.25; $C_{Pdesign}(2c)$=0.19). When it comes to the twist distribution, it can be seen in Figure 11-13, that the lower the TSR_{design} is chosen the bigger the twist close to the root becomes, with an increasing twist at the blade tip. The chord distribution did not change, since the maximum chord was limited to 0.06m and the chord distribution to linear. It has to be mentioned, these designs were not optimized close to the root, but layout with respect to a starting form of a flat plate, to be twisted simply and keeping a slender layout.

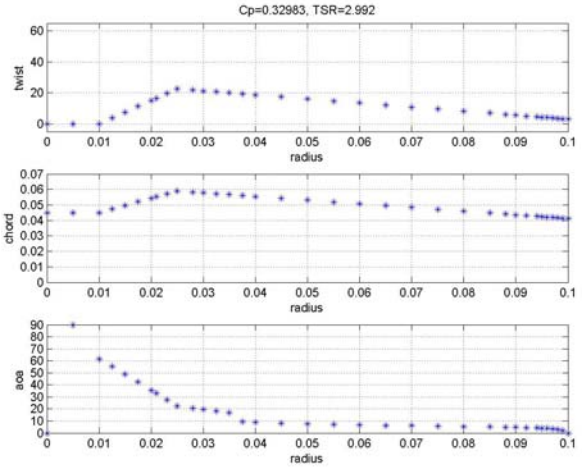

Figure 11: Case 1a); top plot: twist distribution; mid plot: chord distribution; bottom plot: aoa_{design}

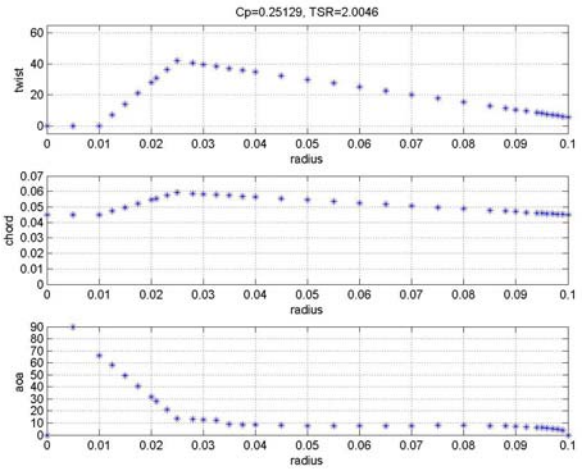

Figure 12: Case 2b); top plot: twist distribution; mid plot: chord distribution; bottom plot: aoa_{design}

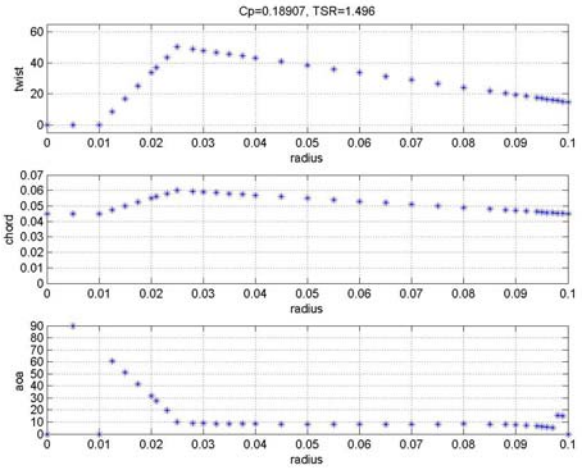

Figure 13: Case 2c); top plot: twist distribution; mid plot: chord distribution; bottom plot: aoa_{design}

Since uncertainties in measurements of the generator characteristics, in the ascertains of airfoil data from xfoil6.96 and uncertainties included in the manufacturing process as well as in the optimization algorithm should be considered, the calculated rotor performance should be higher than the measured generator demand. An easy way to increase the power is to increase the rotor diameter, *d*, ($d^2 \sim P_{shaft}$). And with that we proceed to case three. The settings were as 1a) with modulations

3a) *d*: 0.10m
3b) *d*: 0.25m
3c) *d*: 0.40m

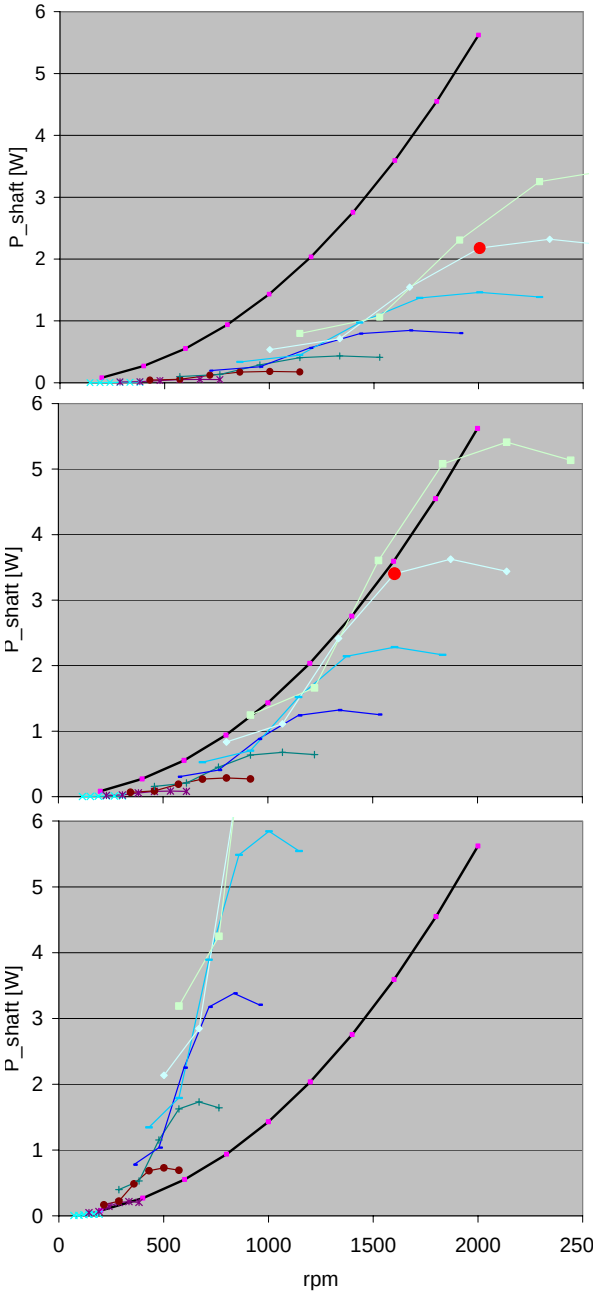

Figure 14: *d* modulation; *P_shaft* over *rpm*

The values for case 3b) and 3c) were obtained by using the C_P values found for the tip speed ratios for case 3a).

$$P_{shaft} = \tfrac{1}{2}\rho v_{wind}^3 A_{rotor} C_P(TSR) \quad TSR = \frac{v_{tip}}{v_{wind}}$$

3 Results

To fit to a bicycle and to be printed with the help of "rapid prototyping" the diameter was set to 0.27m. In order to keep the efficiency in a tolerable range, the design tip speed was chosen to 2.5. Additionally, bigger resistors connected to the generator circuit are considered and plotted in the next *P_shaft*-over-*rpm* charts (-- 14Ohm; __ __ 20Ohm). The bigger the resistor, the lower the necessary power on the shaft gets. These values are theoretical and not evaluated with measurements. Three various final designs were found named 1. BellAIRina, 2. BellAIR, 3. BellAIRphant. For the first one the Cp_{design} was pushed to its maximum design lift and would thereby stall if it experienced wind gusts. The bottom plot of Figure 15 will help to clarify why.

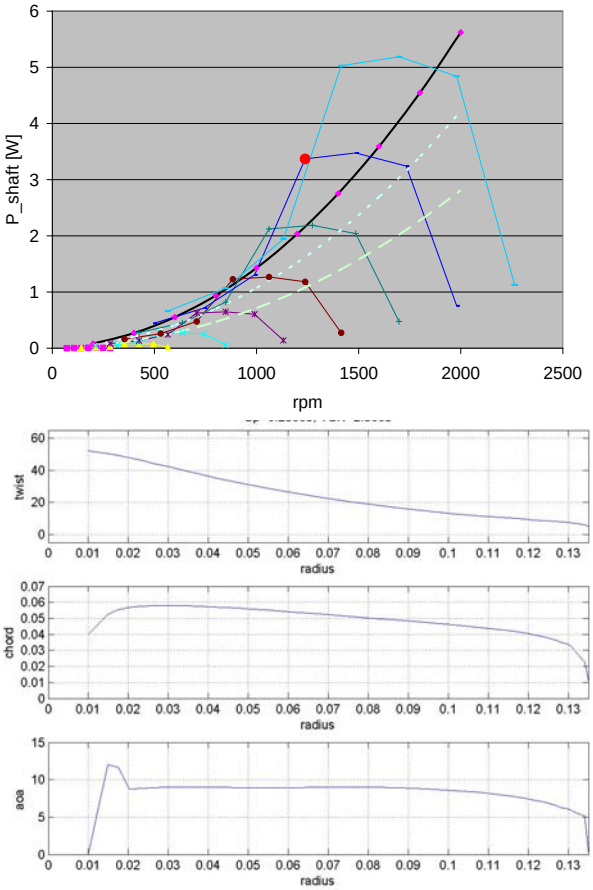

Figure 15: BellAIRina; top plot: *P_shaft* over *rpm*; bottom plot: *twist*, *chord*, aoa_{design} distribution

Here the aoa_{design} is around 9deg over almost the

whole blade. Going back to Figure 2 and following the characteristic for a Reynolds number of 40.000, which is the design point Reynolds number for this geometry, it can be seen that this angle states the point of maximum C_L. As soon as a wind gust increases the angle of attack the blade will stall. That is why the design BellAIR is restricted in its angle of attack to 4.5deg to the cost of $C_{Pdesign}$ (see Figure 16).

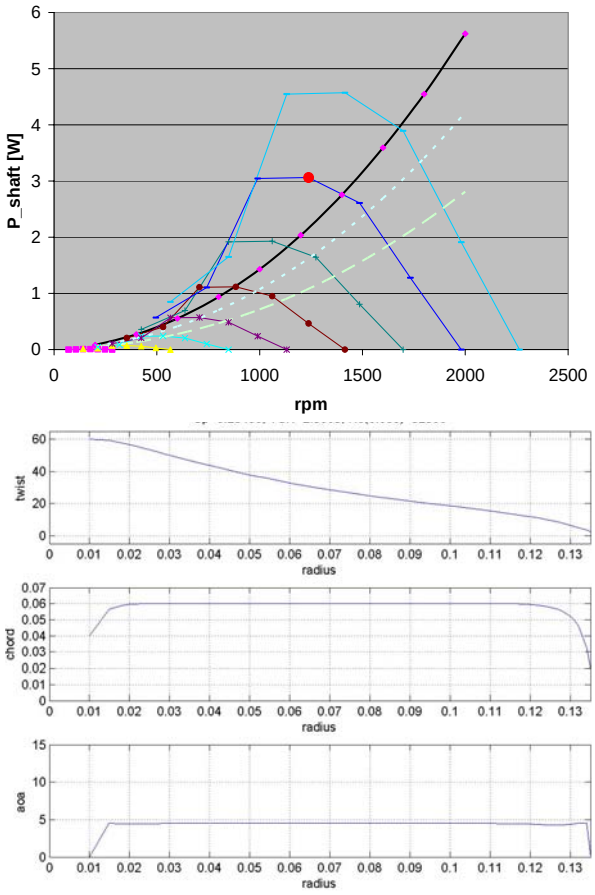

Figure 16: BellAIR; top plot: *P_shaft* over *rpm*; bottom plot: *twist*, *chord*, aoa_{design} distribution

Both designs were subjected to a maximum chord length of 0.06m. If the chord length is free to move the design comes to the third layout, BellAIRphant (see Figure 17).

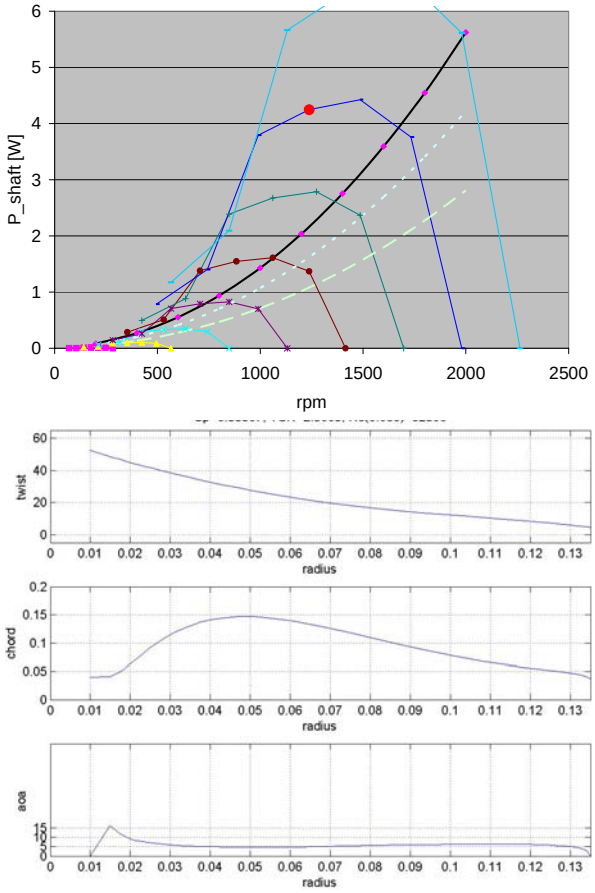

Figure 17: BellAIRphant; top plot: *P_shaft* over *rpm*; bottom plot: *twist*, *chord*, aoa_{design}

To compare the gain in rotor power in the design point, the $C_{Pdesign}$ values are

$C_{Pdesign}$*(BellAIRina)*	=	0.28,
$C_{Pdesign}$*(BellAIR)*	=	0.26,
$C_{Pdesign}$*(BellAIRphant)*	=	0.35.

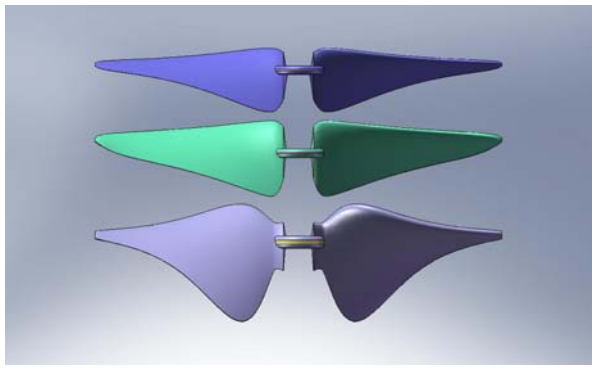

Figure 18: Three dimensional models 1 ; BellAIRina, BellAIR, BellAIRphant

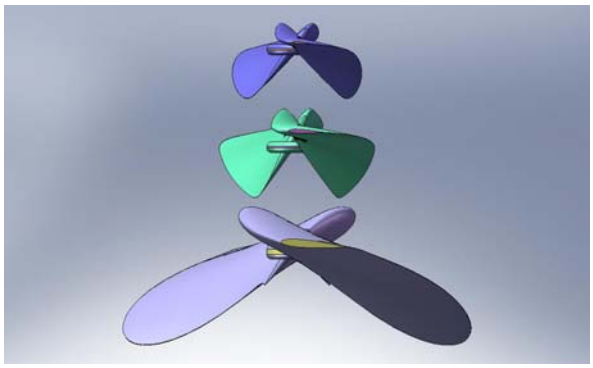

Figure 19: Three dimensional models 2 ; BellAIRina, BellAIR, BellAIRphant

Their properties and applicability are discussed in the next section.

4 Discussion

In the method section was shown how different parameter variations influence the rotor performance. It turned out that a change of the chord distribution from linear to Bezier did not change the outcome significantly. More interesting was the variation of the design tip speed ratio, where the maximum power was shifted to lower rotational speeds and with that closer to the generator line. On the other hand this modification was paid by a less efficient rotor. Pronounced changes were obtained by increasing the rotor diameter, while not changing the power coefficient. These observations lead to a design tip speed ratio of 2.5 and a diameter of 0.27m. In the results chapter three corresponding final designs are presented. For the first model the aerodynamic design was pushed towards maximum lift. With a design angle of attack of 9deg corresponding to the maximum lift coefficient at a Reynolds number of 40.000, it reaches a design power coefficient of 0.28. The second model was designed for an angle of attack of 4.5deg with a change of the power coefficient to 0.26. On the first glance model one seems to have the best performance, but seen on the performance in real wind conditions the second model has the advantage of its capability to take wind gusts better than model one. Both designs were restricted to a max chord length of 0.06m. This limit was chosen for aesthetic reasons. In the third design the chord length was almost free and resulted in a maximum chord of 0.15m and power coefficient of 0.35. Explanation for that is the higher induction in the rotor plane with the big rotor solidity. Comparing Figure 20 with Figure 21 shows an approach of the induction to 0.1 for the second model, bellAIR, whereas the third model, bellAIRphant is close to 0.33, the value for an optimum design.

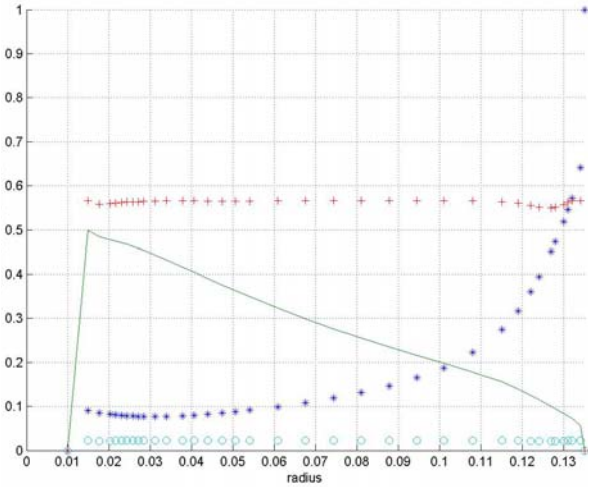

Figure 20: bellAIR; induction (blue star), thrust coefficient (green line), lift coefficient (red cross) and drag coefficient (blue circle) over radius

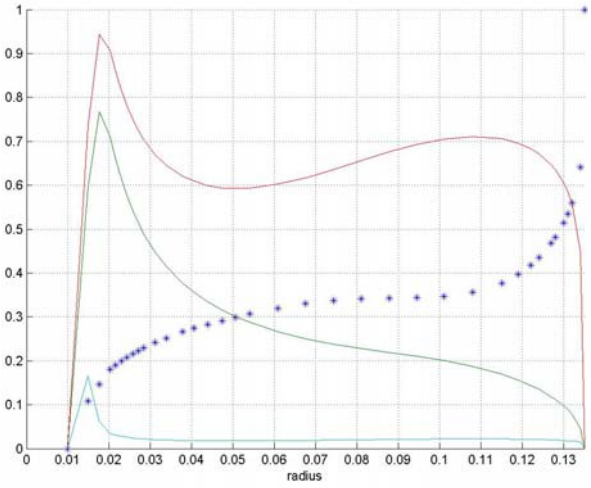

Figure 21: bellAIRphant; induction (blue star), thrust coefficient (green line), lift coefficient (red line) and drag coefficient (blue line) over radius

A higher solidity could have been achieved with more blades as well. Whereas the design was restricted to a two-bladed rotor in order to fit into the diagonal of the three-dimensional printer's volume.

5 Conclusion

The optimum design with the given demands by the generator, safety limit to 2000rpm and dimension limit by the three dimensional printer is BellAIRphant. In the process of printing, though, it turned out that the blades are rather heavy due to the increasing thickness with increasing chord length. Furthermore, it will take more space, see Figure 18. Alternative materials, for example inflatable structures, can make it more

interesting. In general, the generator was over-dimensioned for the diameter limit given by the printer volume. Anyway, for future work the findings shall be evaluated with the rotor models, connected to the generator, exposed to real wind. Investigations for rotors with more than two blades are reasonable and are promising to result in optimum design with shorter chords.

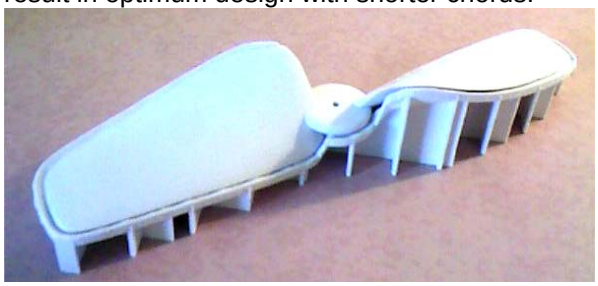

Figure 22: Printed prototyp bellAIRina

Acknowledgements

First of all I would like to say thank you to Andreas Knebel from Faulhaber for the support of hardware and answering questions concerning the motor. Furthermore, thanks to Mads Døssing and Christian Bak for the warm backup. And last but not least, thanks to Steen Markvorsen for the printer support and friendly instructions.

References

[1] Fuglsang P. and Thomsen, K., 2001, Site Specific Design Optimization Of Wind Turbines. ASME J. Solar Engineering,Vol. 123, pp 296-303

[2] Drela M. XFOIL, An Analysis and Design system for Low Reynolds Number Airfoils. Low Reynolds Number Aerodynamics, volume 54. In Springer- Verlag Lec. Notes in Eng., 1989

Motor data sheet

FAULHABER

DC-Kleinstmotoren — 50 mNm

Graphitkommutierung

Kombinierbar mit (Übersicht Seiten 14-15)
Getriebe:
30/1, 32/3, 38/1, 38/2
Impulsgeber:
5500, 5540

Serie 3557 ... CS

		3557 K		009 CS	012 CS	020 CS	024 CS	048 CS	
1	Nennspannung	U_N		9	12	20	24	48	Volt
2	Anschlusswiderstand	R		0,70	1,34	4,0	5,5	23,0	Ω
3	Abgabeleistung	$P_{2\,max.}$		28,1	26,1	24,3	25,4	24,1	W
4	Wirkungsgrad	$\eta_{max.}$		78	79	79	78	76	%
5	Leerlaufdrehzahl	n_o		5 700	5 400	5 500	5 500	5 200	rpm
6	Leerlaufstrom (bei Wellen ø 4,0 mm)	I_o		0,190	0,125	0,070	0,065	0,040	A
7	Anhaltemoment	M_H		188	185	169	176	177	mNm
8	Reibungsdrehmoment	M_R		2,80	2,60	2,40	2,70	3,50	mNm
9	Drehzahlkonstante	k_n		643	456	279	233	110	rpm/V
10	Generator-Spannungskonstante	k_E		1,560	2,190	3,590	4,300	9,050	mV/rpm
11	Drehmomentkonstante	k_M		14,90	20,90	34,20	41,00	86,50	mNm/A
12	Stromkonstante	k_I		0,067	0,048	0,029	0,024	0,012	A/mNm
13	Steigung der n-M-Kennlinie	Δn/ΔM		30,3	29,2	32,5	31,3	29,4	rpm/mNm
14	Anschlussinduktivität	L		100	220	630	850	3 400	µH
15	Mechanische Anlaufzeitkonstante	τ_m		16	16	16	16	16	ms
16	Rotorträgheitsmoment	J		50	52	47	49	52	gcm²
17	Winkelbeschleunigung	$\alpha_{max.}$		37	35	36	36	34	$\cdot 10^3$rad/s²
18	Wärmewiderstände	$R_{th\,1}$ / $R_{th\,2}$		1,5 / 9					K/W
19	Thermische Zeitkonstante	τ_{w1} / τ_{w2}		15 / 900					s
20	Betriebstemperaturbereich:								
	– Motor			– 30 ... + 125					°C
	– Rotor, max. zulässig			+ 125					°C
21	Wellenlagerung			Kugellager, vorgespannt					
22	Wellenbelastung, max. zulässig:								
	– für Wellendurchmesser			4,0					mm
	– radial bei 3 000 rpm (3 mm vom Lager)			30					N
	– axial bei 3 000 rpm			5					N
	– axial im Stillstand			50					N
23	Wellenspiel:								
	– radial		≤	0,015					mm
	– axial		=	0					mm
24	Gehäusematerial			Stahl, galvanisch verzinkt, passiviert					
25	Gewicht			275					g
26	Drehrichtung			rechtsdrehend auf Abtriebswelle gesehen					
Empfohlene Werte - diese gelten unabhängig voneinander									
27	Drehzahl bis	$n_{e\,max.}$		5 000	5 000	5 000	5 000	5 000	rpm
28	Dauerdrehmoment bis [1]	$M_{e\,max.}$		50	50	50	50	50	mNm
29	Thermisch zulässiger Dauerstrom	$I_{e\,max.}$		3,150	2,260	1,300	1,100	0,540	A

[1] Wärmewiderstand $R_{th\,2}$ um 40% reduziert